IEEE Photonics Journal
An IEEE Photonics Society Publication

Open Access

# Reconfigurable Chiral Metasurface Absorbers Based on Liquid Crystals

Volume 10, Number 6, December 2018

Shengtao Yin
Dong Xiao
Jianxun Liu
Ke Li
Huilin He
Shouzhen Jiang
Dan Luo
Xiao Wei Sun
Wei Ji
Yan Jun Liu

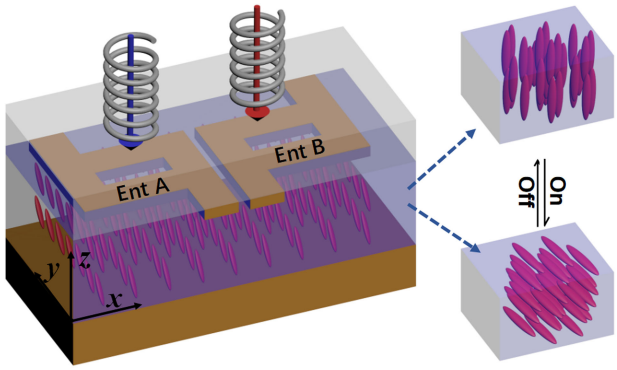


DOI: 10.1109/JPHOT.2018.2878775
1943-0655 

# Reconfigurable Chiral Metasurface Absorbers Based on Liquid Crystals

**Shengtao Yin,[1,2] Dong Xiao,[1] Jianxun Liu,[1] Ke Li,[1] Huilin He,[1] Shouzhen Jiang,[3] Dan Luo,[1] Xiao Wei Sun,[1,4] Wei Ji,[2] and Yan Jun Liu [1,4]**

[1]Department of Electrical and Electronic Engineering, Southern University of Science and Technology, Shenzhen 518055, China
[2]School of Information Science and Engineering, Shandong University, Jinan 250000, China
[3]School of Physics and Electronics, Shandong Normal University, Jinan, 250014, China
[4]Shenzhen Planck Innovation Technologies Pte. Ltd., Shenzhen 518112, China

*DOI:10.1109/JPHOT.2018.2878775*


Manuscript received October 2, 2018; revised October 23, 2018; accepted October 27, 2018. Date of publication November 1, 2018; date of current version November 13, 2018. This work was supported by the National Natural Science Foundation of China under Grants 61805113 and 61571273, in part by the Natural Science Foundation of Guangdong Province under Grants 2017A030313034 and 2018A030310224, in part by the Shenzhen Science and Technology Innovation Commission under Grants JCYJ20170817111349280 and KQTD2016030111203005, and in part by the Guangdong Innovative and Entrepreneurial Research Team Program under Grant 2017ZT07C071. Corresponding authors: Wei Ji and Yan Jun Liu (e-mail: jiwww@sdu.edu.cn; yjliu@sustc.edu.cn).

**Abstract:** We propose a liquid-crystal-based reconfigurable chiral metasurface absorber and numerically investigate its chiro-optical properties. The chiral metasurface absorber consists of a metal–insulator–metal structure with the substrate, which can strongly absorb a circularly polarized wave of one spin state and reflects that of the opposite spin, resulting a strong circular dichroism (CD). A birefringent liquid crystal (LC) is exploited to serve as the insulator layer in the metal–insulator–metal structure. We could then vary the circular state of the incident light by controlling the alignment of the LC molecules, hence inversing the CD. The simulation results show that the CD will change the sign as the LC molecules are realigned from 0° to 90°. The absorption efficiency for the specific circularly polarized wave is larger than 80% and the CD is nearly 70%. The simple and compact design of our proposed chiral metasurface absorber is especially favorable for integration, and such a reconfigurable chiral absorber could find many potential applications in biological detection/sensing, polarimetric imaging, and optical communications.

**Index Terms:** Chirality, metasurface, absorber, liquid crystals, reconfigurability.

## 1. Introduction

Just like the wavelength, intensity, and phase, the circular polarization state of light also plays an important role in light-matter interactions. The electric field vector of a circularly polarized light (CPL) beam travels along a helical trajectory by either clockwise or counterclockwise, corresponding to the left-handed circular polarization (LCP) or right-handed circular polarization (RCP). As known, a CPL beam can be decomposed into two linearly polarized light waves with a 90° phase shift [1]. However, owing to the lack of the intrinsic chirality for conventional photodetectors, it's not easy to differentiate the above mentioned two circular polarization states. Chirality refers to an object's geometry lacking any mirror symmetry plane. The intrinsic chirality inside a material plays a critical role in many chiro-optical phenomena, such as circular dichroism (CD) [2], optical rotatory

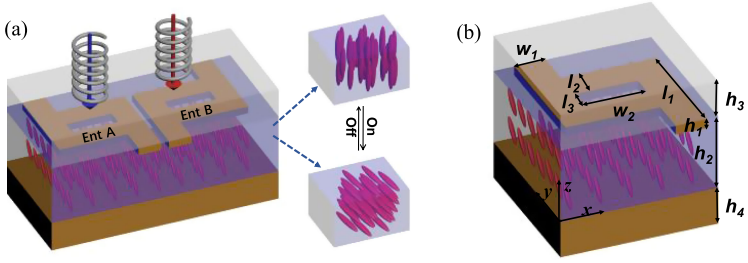


Fig. 1. (a) Schematic diagram of the chiral metasurface absorber composed of a semi-infinite $SiO_2$ claddings, two L- or inverse L-shaped gold nanohole arrays, a LC-filled dielectric layer in the middle of the MIM structure and a gold mirror in the bottom. The pair enantiomers of the chiral metasurface that are labelled as Ent A and Ent B, respectively. The important geometrical parameters are defined in (b).

dispersion and Raman optical activity. CD is of vital importance in the chemical and biomolecular structural characterization and spectroscopy. However, the interaction between light and chiral molecules is usually very weak, resulting in weak CD signals. To overcome this issue, researchers have proposed many artificially designed chiral nanostructures (often described as metamaterials or metasurfaces) to enhance the CD, such as helix [3], oligomers [4], twisted metamaterials [5]–[7] fish-scale metamaterials [8], spiral [9], Z-shaped chiral structures [10], [11], and so on. A few of these artificial metamaterials have been utilized to enhance chiral-selective field or detect the photocurrent [12]. Therefore, we can see that the interaction of CPL and chiral metasurfaces would play a crucial role for the plasmonic circularly polarized absorbers. Nevertheless, most chiral absorbers demonstrated so far are at gigahertz [13]–[15] and terahertz [16], [17] frequencies. Furthermore, most of the aforementioned chiral metasurface absorbers are passive and their performance is only determined by their designed configuration. As a result, it is impossible to reconfigure the device without redesigning and repeating the entire fabrication processes. This will put a big hurdle for the future development that requires both passive and active devices. In this regard, it is highly desirable to develop actively reconfigurable metasurface absorbers that could be better suit the actual needs. For instance, the fine tuning of the absorption band via active control (i.e., external stimuli) could maximize the absorption efficiency at the desired wavelength range, which is hardly to achieve without experimental optimization due to the fabrication errors. The active tuning could significantly save labor and fabrication cost. Thus far, a few studies have emerged based on the active media, such as electro-optics, nonlinear optics, or gain material. Among them, liquid crystals (LCs) stand out due to their two main distinctive advantages: a) the fluid nature of LCs that provides great flexibility in device configurations and geometries; b) the fast response speed at millisecond (or even microsecond) scale that is usually faster than most conventional electro-optics devices. In addition, LCs also have low driving threshold, large birefringence and versatile driving methods, which are particularly favourable for active plasmonics [18], [19]. Up to now, both electrical [20]–[27] and optical tuning [28]–[31] of plasmonic properties have been demonstrated by utilizing the LC molecules' reorientation.

In this paper, we propose and demonstrate theoretically a reconfigurable chiral metasurface absorber in the near-infrared range. The proposed chiral metasurface absorber has a highly spin-selective absorption behavior, meaning that it can almost absorb one designated CPL state and reflect the other opposite state. By controlling the alignment of the insulator (LCs) from 0° to 90°, the reflecting and absorbing behaviors can be completely flipped, hence resulting in an inversed CD as well. Such novel reconfigurable absorbers could find many potential applications in chirality detection/sensing, polarimetric imaging, and spin-orbit communications.

## 2. Structure and Theoretical Analysis

Fig. 1 schematically depicts the structural configuration of the proposed chiral metasurface absorber. The chiral absorber is sandwiched with a metal-insulator-metal (MIM) structure on the quartz

substrates. The building block unit consists of two L-shaped metallic resonators and a metallic mirror that are on top and bottom of the insulator layer, respectively. We exploit an active, anisotropic medium to serve as the insulator layer, which is a birefringent, nematic LC in our proposed chiral absorber. The refractive index of the used LCs can be tuned from 1.52 to 1.72 [32]. The incoming LCP or RCP light within the wavelength range of 900–1000 nm is normally incident onto the top side of the chiral metasurface. It is worth mentioning that in this simulation we have ignored the alignment layer of the LCs since the alignment layer is only few to few tens of nanometers thick.

As known, the electric field vector of the CPL can be decomposed into two orthogonally linearly polarized electric fields, which have a 90° phase difference [1]:

$$E_{RCP} = (E_x, E_y)^T = \left(\frac{\sqrt{2}}{2}, \frac{\sqrt{2}}{2} e^{\frac{\pi}{2} i}\right)^T \tag{1}$$

$$E_{LCP} = (E_x, E_y)^T = \left(\frac{\sqrt{2}}{2}, \frac{\sqrt{2}}{2} e^{-\frac{\pi}{2} i}\right)^T \tag{2}$$

The equations show that the phase of $E_x$ is 90° behind of $E_y$ for the case of LCP and 90° ahead of $E_y$ for the case of RCP. Hence, we can further analyze the necessary condition to select the reflection for one designed state of circular polarization based on advanced Jones calculus. The incident and reflected fields can be related by reflection matrix $R$ via advanced Jones calculus [33]:

$$\begin{bmatrix} E_r^x \\ E_r^y \end{bmatrix} = \begin{bmatrix} r_{xx} & r_{xy} \\ r_{yx} & r_{yy} \end{bmatrix} \begin{bmatrix} E_i^x \\ E_i^y \end{bmatrix} = R \begin{bmatrix} E_i^x \\ E_i^y \end{bmatrix} \tag{3}$$

where $E_i^x$ and $E_r^x$ are the incident and reflected electric fields for the $x$-polarized direction, respectively. The $y$-polarized direction is in a similar fashion. The reflection matrix $R_c$ for a circular polarization state is as follows [34]:

$$\begin{aligned} R_c &= \begin{bmatrix} r_{++} & r_{+-} \\ r_{-+} & r_{--} \end{bmatrix} = \frac{1}{2} \begin{bmatrix} 1 & 1 \\ i & -i \end{bmatrix} R \begin{bmatrix} 1 & 1 \\ i & -i \end{bmatrix} \\ &= \frac{1}{2} \begin{bmatrix} r_{xx} + r_{yy} + i(r_{xy} - r_{yx}) & r_{xx} - r_{yy} - i(r_{xy} + r_{yx}) \\ r_{xx} - r_{yy} + i(r_{xy} + r_{yx}) & r_{xx} + r_{yy} - i(r_{xy} - r_{yx}) \end{bmatrix} \end{aligned} \tag{4}$$

$$R_c = \begin{bmatrix} r_{++} & r_{+-} \\ r_{-+} & r_{--} \end{bmatrix} = \begin{bmatrix} r_{LR} & r_{LL} \\ r_{RR} & r_{RL} \end{bmatrix} \tag{5}$$

From Eqs. (4) and (5), the '+' and '−' are defined as the clockwise and counterclockwise CPL with the view along $+z$-direction, respectively. And the reflection coefficient $r_{LL}$ ($r_{RL}$) is defined as the LCP (RCP) portion of the reflected light from the metasurface to that of the LCP light incidence, while $r_{RR}$ ($r_{LR}$) represents the corresponding inverse conversion of circular polarization. Thus, we can obtain all components of the RCP and LCP light from the plane wave. This working principle of the proposed chiral metasurface absorber is well carried out in our simulations, which is performed using the finite-difference time-domain (FDTD) method [35].

As known, a phase delay will be induced as the CPL propagates in the birefringent LCs that will change the polarization state. The phase delay satisfies the following equation [36]:

$$\Delta\varphi = 2\pi h \Delta n / \lambda \tag{6}$$

where $\Delta\varphi$ is the phase difference, $\lambda$ is the wavelength of the incident light, $h$ is the height of the LC [i.e., $h_2$ in Fig. 2(b)] and $\Delta n$ is the absolute value of the LC's birefringence.

## 3. Simulation Results and Analysis

In this paper, we define the CD as CD $= |A_{LCP} - A_{RCP}|$ which characterizes the absorbance difference between LCP and RCP. Since the thickness of the gold mirror layer is much larger than its

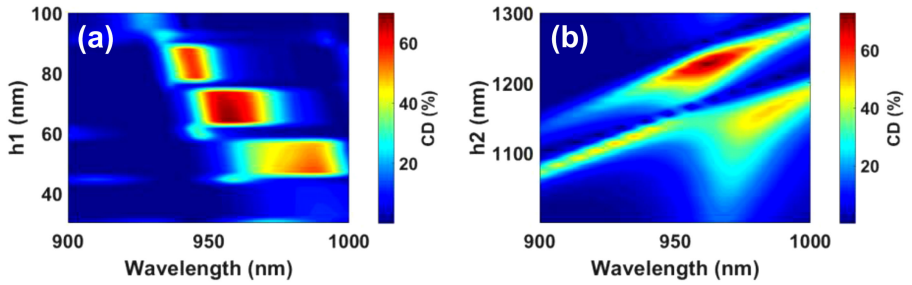


Fig. 2. CD as a function of the thickness of the (a) top gold and the (b) LC layers under CPL illumination, respectively.

skin depth, the transmittance can be assumed to be zero. As a result, the CD can be also written as $\mathrm{CD} = |R_{LCP} - R_{RCP}|$. For the enantiomer A and B, we can choose to obtain LCP or RCP light.

It is straightforward that the geometric parameters of the designed nanostructure will have a strong impact on the chiral absorption properties. Fig. 2(a) and 2(b) respectively show the calculated CD as a function of the thickness of the gold top-layer $h_1$ and the LC layer $h_2$ in our interested wavelength range under the CPL illumination. We can see from Fig. 2 that the chiroptical resonance is strongly dependent on the thickness of the gold nanostructure and LC layer. It is understandable that the change of the thickness of the top gold nanostructure layer will lead to the wavelength shifting of the plasmonic resonance. Only in certain wavelength range, the light with the wavelength not only coinciding with the plasmonic resonance but also undergoing an exact $\pi$ phase retardation, we can achieve the strongest CD. As a result, we observe a step-like behavior of the CD in Fig. 2(a) when we change the thickness of the gold nanostructure. Given the ease of fabrication, we have optimized the geometrical parameters of our design as the following in Fig. 1(b): $w_1 = 40\,\mathrm{nm}$, $w_2 = 52\,\mathrm{nm}$, $l_1 = 200\,\mathrm{nm}$, $l_2 = 90\,\mathrm{nm}$, $l_3 = 36\,\mathrm{nm}$, $h_1 = 63\,\mathrm{nm}$, $h_2 = 1220\,\mathrm{nm}$, $h_3 = 1000\,\mathrm{nm}$, $h_4 = 100\,\mathrm{nm}$. The thickness of the gold mirror should be over its skin depth, which can guarantee to reflect all the incident light back. The period along the *x*- and *y*-axis are $p_x = 200\,\mathrm{nm}$ and $p_y = 300\,\mathrm{nm}$, respectively.

With the given geometrical parameters, we further numerically investigate the chiroptical responses of the enantiomers A and B using the FDTD method. The entire structure was fully surrounded by air. The single unit metasurface nanostructure was simulated with periodic (*x*- and *y*-directions) and perfectly matched layer (PML) (*z*-direction) boundary conditions. The refractive index of the quartz substrate is 1.46. And the refractive index of the gold can be well described by the Johnson and Christy model [37]. A maximum mesh size of 5 nm was set for the simulation to ensure the calculation accuracy. The simulation results are shown in Fig. 3. Fig. 3(a) and 3(b) show the circular polarization-dependent refection and CD of enantiomers A and B, respectively. We can see the enantiomers A and B have a strong CD response at the wavelength of ~960 nm with the horizontal alignment of LCs. For either case, one spin state of circular polarization can be reflected more than 70%, while the opposite spin state can be absorbed over 80% by the hybrid MIM system. The achieved CD from the simulation is ~70%, which is much higher than the reported work [15]. It is worth mentioning that the top gold nanostructure layer itself has no chiroptic effect due to the geometric symmetry. The CD effect in this system mainly results from the phase retardation caused by the LC layer.

To further understand the corresponding reflecting behavior, we carried out a detailed analysis regarding the LCP and RCP components (i.e., $r_{LL}$, $r_{RL}$, $r_{RR}$, and $r_{LR}$) of the reflection spectrum for enantiomer A and B, as shown in Fig. 3(c) and 3(d). We could only observe three calculated curves for the reason of $r_{LR} = r_{RL}$. For the designed nanostructure which possesses the mirror symmetry along the *z*-axis, it satisfies the following equation [33]:

$$R_c = \frac{1}{2}\begin{bmatrix} r_{xx} + r_{yy} & r_{xx} - r_{yy} + 2ir_{xy} \\ r_{xx} - r_{yy} - 2ir_{xy} & r_{xx} + r_{yy} \end{bmatrix} = \begin{bmatrix} r_{LR(RL)} & r_{LL} \\ r_{RR} & r_{RL(LR)} \end{bmatrix} \tag{7}$$

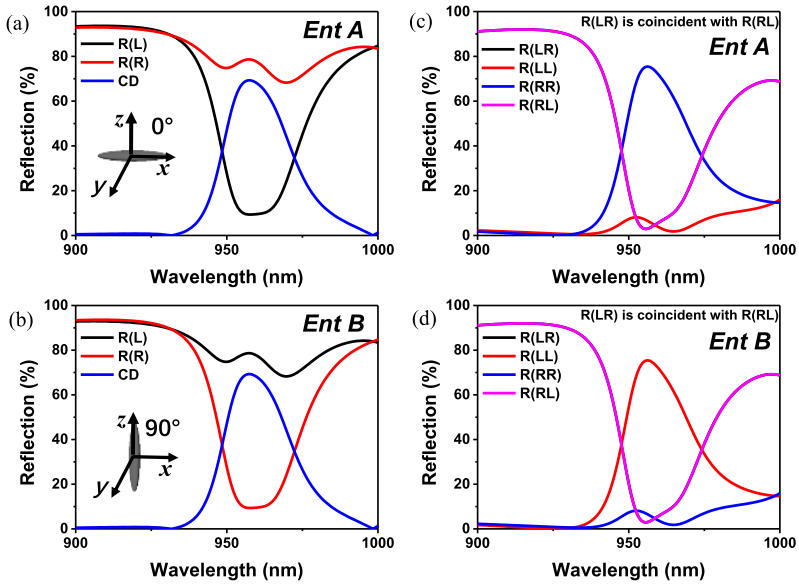


Fig. 3. Simulated reflection and CD spectra of the chiral metasurface absorber for (a) Ent A and (b) B. The reflection spectra of (c) Ent A and (d) B for the LCP and RCP components. The alignment of the LC molecules is assumed to be horizontal.

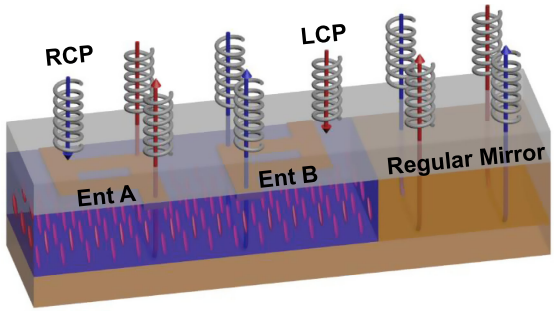


Fig. 4. Schematic of the reflection behaviors of the chiral absorber and a regular mirror. The chiral absorber composed of Ent A (B) reflects LCP (RCP) incident light and absorbs the entire RCP (LCP) component.

From Fig. 3(c) and 3(d), we can see that the cross-polarization conversion for LCP or RCP ($r_{RL}$, $r_{LR}$) tends to be zero at the resonant wavelength. The reflection and absorption result mainly from $r_{LL}$ and $r_{RR}$. To have an intuitive picture about the working principle of the metasurface, a comparative schematic drawing is illustrated in Fig. 4. As seen from Fig. 4, for regular metallic mirrors, an incoming CPL will completely reverse its spin state upon reflection ($r_{LR} = r_{RL} \asymp 100\%$, $r_{LL} = r_{RR} \asymp 0$). By comparison, the metasurface with the structure Ent A (B) will maintain its initial state of circular polarization upon reflection. For Ent A (B), the incident LCP (RCP) light still keeps it original spin state upon reflection, while the incident light with the opposite RCP (LCP) is largely absorbed. These reflecting and absorbing behaviors can be attributed to the tailored, strong light-matter interaction between the CPL and the designed metasurface nanostructures.

A distinctive advantage is that our proposed chiral metasurface absorber is reconfigurable by replacing the passive insulator layer with an active LC layer. As a result, we can tune the designed device to absorb either LCP or RCP via externally controlling the alignment of the LC molecules. Taking the structure Ent A as an example. In this work, the designed metasurface essentially utilizes the plasmonic resonances of the gold enantiomer nanostructures. It is well known that the

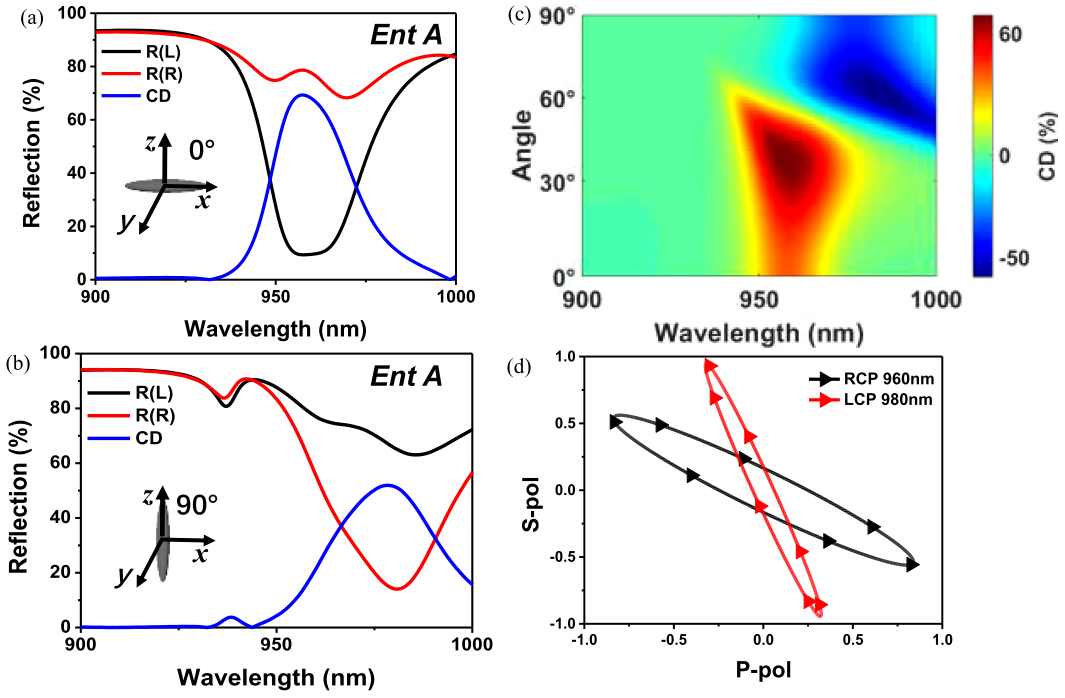


Fig. 5. (a), (b) Simulated reflection and CD spectra of the chiral metasurface absorber with the LC alignmnet being horizontal (0°) and vertical (90°), respectively. (c) CD as a function of LCs' alignment under CPL illumination. (d) The polarization states of the reflected light under CPL illumination for the horizontal (0°) alignment at the resonance position of $\lambda = 960$ nm and vertical (90°) alignment at the resonance position of $\lambda = 980$ nm, respectively.

plasmonic resonance is highly sensitive to the dielectric properties of the surrounding medium [38]. In our design, a widely used LC E7 [39] is exploited to serve as the insulator layer of the MIM system. The LC E7 has a birefringence of $\Delta n = 0.2253$ which its ordinary refractive index of $n_o = 1.5211$ and extraordinary refractive index of $n_e = 1.7464$ at 20 °C. Considering the general strong anchoring at the interfaces, we assume that the birefringence of the LC is $n_o = 1.52$ and $n_e = 1.72$ in our simulation. The orientation of the LC molecules can be controlled by applying voltage to the conductive gold mirror. From Eq. (6), in order to inverse the LCP to RCP (or RCP to LCP) in the LC cavity, we need to set $\Delta\varphi$ as $\pi$. The absorbed wavelength $\lambda$ is 960nm. Hence, we can calculate and optimize the thickness of the LC layer to be 2440 nm. Given the reflection process, the height of the LC layer needs only half of the total thickness, i.e., $h_2 = 1220$ nm [Fig. 2(b)].

Fig. 5(a) and 5(b) show the simulated reflection and CD spectra of the chiral metasurface absorber for an incident CPL at the homogeneous (horizontal) and homeotropic (vertical) alignment of LC molecules, respectively. The resulted CD spectrum with the change of the LC molecules' tilting angle is also depicted in Fig. 5(c). The observed sharp change of the CD value in Fig. 5(c) is the result of the sign change of the CD, which happens at the ~60° tilting angle of LC molecules. We can clearly see that the CD changes its sign from positive to negative when the tilting angle increases, meaning that the inversion of the spin state of the incident CPL takes place inside the LC layer, leading to absorption of the opposite CPL, which can be clearly observed from Fig. 5(a) and 5(b). In addition, we can also see that the CD peak (corresponding absorption peak as well) red-shifts from 960 nm to 980 nm as the alignment changes from homogeneous to homeotropic. This is mainly attributed to the change of the LC's effective refractive index by the alignment, which further affects the plasmonic resonances of the metasurface nanostructure. Fig. 5(d) shows the polarization ellipse of the reflected light at the wavelengths of the CD peaks at the homogeneous and homeotropic alignment of LC molecules, respectively. It is worth mentioning that the homogeneous

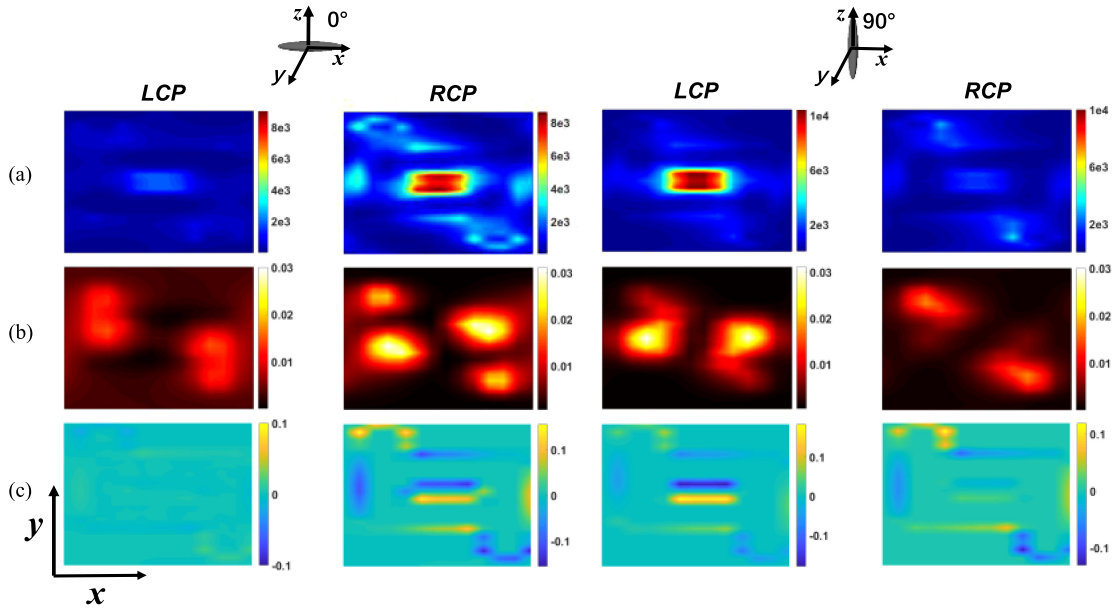


Fig. 6. Simulated (a) electric field, (b) magnetic field, and (c) charge distributions at the absorption peak position for Ent A under RCP and LCP illumination with horizontal and vertical alignment of LCs, respectively.

and homeotropic alignment can be easily realized by applying an external electric field on the LC layer.

The circular polarization-dependent light absorption and chiro-optical responses can be ascribed to the excitation of different plasmonic resonance modes in the metasurface. To clearly reveal the physical origins, the electric field, magnetic field, and charge distributions were calculated at the resonance positions for both alignment cases. Fig. 6 shows the calculated results at the Au nanostructure-LC interface. It is obvious that strong electromagnetic fields are located about the nanostructured Au for the incident CPL, which are also highly dependent on the CPL spin state. The chiroptical responses stem from the magnetic dipoles excited by the electric field component of light [40]. We attribute this strong electromagnetic field and current distribution to the enhancement of localized surface plasmon resonance at the metal (Au)–dielectric (LCs) interface, which causes to the specific absorption. Compared to the electric fields with the 0° and 90° alignment of LCs, they are almost identical for the CPL illumination with two opposite spin states. The little difference is attributed to the effect of the LC molecules' different orientation and the different refractive index. The reflection between the gold mirror and gold structure also enhance the specific CPL absorption. This actively controlled MIM system gives one great freedom to finely tune the CD/absorption/reflection spectrum to the specific CPL without redesigning and repeating the entire fabrication processes.

## 4. Conclusion

In summary, we have demonstrated a reconfigurable chiral metasurface absorber consisting of a MIM structure with the substrates. The metasurface absorber can strongly absorb a CPL of one spin state and reflects that of the opposite spin in the near-infrared range. With a LC medium serving as the insulator layer, we can then make the metasurface absorber reconfigurable by externally controlling the LC alignment. The simulation results have shown that the reconfigurable chiral metasurface absorber has excellent performance with $>$70% refection, $>$80% absorption and $\sim$70% CD for CPL incidence. More importantly, the CD of the proposed system can change its sign reversibly in between the homogeneous and homeotropic states of the LC layer. The design of the

proposed metasurface absorber is simple and compact, which is favorable for easy fabrication and integration. Such reconfigurable chiral metasurface absorbers could find many potential applications in biological detection/sensing, polarimetric imaging, and optical communication.

## References


[1] A. K. Jin, *Research Topics in Electromagnetic Wave Theory*. Hoboken, NJ, USA: Wiley, 1981.
[2] B. Nordén, *Linear Dichroism and Circular Dichroism* (Encyclopedia of Analytical Chemistry). Hoboken, NJ, USA: Wiley, 2010.
[3] J. K. Gansel, M. Thiel, M. S. Rill, M. Decker, K. Bade, and V. Saile, "Gold helix photonic metamaterial as broadband circular polarizer," *Science*, vol. 325, pp. 1513–1515, 2009.
[4] B. Hopkins, A. N. Poddubny, A. E. Miroshnichenko, and Y. S. Kivshar, "Circular dichroism induced by Fano resonances in planar chiral oligomers," *Laser Photon. Rev.*, vol. 10, pp. 137–146, 2016.
[5] Y. Zhao, A. N. Askarpour, L. Sun, J. Shi, X. Li, and A. Alù, "Chirality detection of enantiomers using twisted optical metamaterials," *Nature Commun.*, vol. 8, 2017, Art. no. 14180.
[6] Y. Cui, L. Kang, S. Lan, S. Rodrigues, and W. Cai, "Giant chiral optical response from a twisted-arc metamaterial," *Nano Lett.*, vol. 14, pp. 1021–1025, 2014.
[7] M. Hentschel, M. Schäferling, T. Weiss, N. Liu, and H. Giessen, "Three-dimensional chiral plasmonic oligomers," *Nano Lett.*, vol. 12, pp. 2542–2547, 2012.
[8] V. A. Fedotov, A. S. Schwanecke, N. I. Zheludev, V. V. Khardikov, and S. L. Prosvirnin, "Asymmetric transmission of light and enantiomerically sensitive plasmon resonance in planar chiral nanostructures," *Nano Lett.*, vol. 7, pp. 1996–1999, 2007.
[9] F. Afshinmanesh, J. S. White, W. Cai, and M. L. Brongersma, "Measurement of the polarization state of light using an integrated plasmonic polarimeter," *Nanophotonics*, vol. 1, pp. 125–129, 2012.
[10] W. Li, Z. J. Coppens, L. V. Besteiro, W. Wang, A. O. Govorov, and J. Valentine, "Circularly polarized light detection with hot electrons in chiral plasmonic metamaterials," *Nature Commun.*, vol. 6, 2015, Art. no. 8379.
[11] L. Kang, S. P. Rodrigues, M. Taghinejad, S. Lan, K. T. Lee, and Y. Liu, "Preserving spin states upon reflection: Linear and nonlinear responses of a chiral meta-mirror," *Nano Lett.*, vol. 17, pp. 7102–7109, 2017.
[12] C. R. Han and W. Y. Tam, "Broadband optical magnetism in chiral metallic nanohole arrays by shadowing vapor deposition," *Appl. Phys. Lett.*, vol. 109, 2016, Art. no. 251102.
[13] L. Jing, Z. Wang, Y. Yang, B. Zheng, Y. Liu, and H. Chen, "Chiral metamirrors for broadband spin-selective absorption," *Appl. Phys. Lett.*, vol. 110, 2017, Art. no. 231103.
[14] J. Wang, Z. Shen, and W. Wu, "Broadband and high-efficiency circular polarizer based on planar-helix chiral metamaterials," *Appl. Phys. Lett.*, vol. 111, 2017, Art. no. 113503.
[15] E. Plum, "Extrinsic chirality: Tunable optically active reflectors and perfect absorbers," *Appl. Phys. Lett.*, vol. 108, 2016, Art. no. 241905.
[16] D. Hay, Y. Ye, and Z. Shi, "Coherent perfect absorption in chiral metamaterials," *Opt. Lett.*, vol. 41, pp. 3359–3362, 2016.
[17] S. Zhang, J. Zhou, Y. S. Park, J. Rho, R. Singh, and S. Nam, "Photoinduced handedness switching in terahertz chiral metamolecules," *Nature Commun.*, vol. 3, 2012, Art. no. 942.
[18] G. Y. Si, Y. H. Zhao, E. S. P. Leong, and Y. J. Liu, "Liquid-crystal-enabled active plasmonics: A review," *Materials*, vol. 7, pp. 1296–1317, 2014.
[19] I. C. Khoo, "Nonlinear optics, active plasmonics and metamaterials with liquid crystals," *Prog. Quantum Electron.*, vol. 38, pp. 77–117, 2014.
[20] P. A. Kossyrev *et al.*, "Electric field tuning of plasmonic response of nanodot array in liquid crystal matrix," *Nano Lett.*, vol. 5, pp. 1978–1981, 2005.
[21] Y. J. Liu, E. S. P. Leong, B. Wang, and J. H. Teng, "Optical transmission enhancement and tuning by overlaying liquid crystals on a gold film with patterned nanoholes," *Plasmonics*, vol. 6, pp. 659–664, 2011.
[22] Y. J. Liu, Q. Hao, J. S. T. Smalley, J. Liou, I. C. Khoo, and T. J. Huang, "A frequency-addressed plasmonic switch based on dual-frequency liquid crystals," *Appl. Phys. Lett.*, vol. 97, 2010, Art. no. 091101.
[23] W. Dickson, G. A. Wurtz, P. R. Evans, R. J. Pollard, and A. V. Zayats, "Electronically controlled surface plasmon dispersion and optical transmission through metallic hole arrays using liquid crystal," *Nano Lett.*, vol. 8, pp. 281–286, 2008.
[24] J. Muller, C. Sonnichsen, H. V. Poschinger, G. V. Plessen, T. A. Klar, and J. Feldmann, "Electrically controlled light scattering with metal nanoparticles," *Appl. Phys. Lett.*, vol. 81, pp. 171–173, 2003.
[25] K. C. Chu, C. Y. Chao, Y. F. Chen, Y. C. Wu, and C. C. Chen, "Electrically controlled surface plasmon resonance frequency of gold nanorods," *Appl. Phys. Lett.*, vol. 89, 2006, Art. no. 103107.
[26] S. T. Yin *et al.*, "Liquid-crystal-based tunable plasmonic waveguide filters," *J. Phys. D, Appl. Phys.*, vol. 51, 2018, Art. no. 235101.
[27] D. Xiao *et al.*, "Liquid-crystal-loaded chiral metasurfaces for reconfigurable multiband spin-selective light absorption," *Opt. Exp.*, vol. 26, pp. 25305–25314, 2018.
[28] Y. J. Liu, Y. B. Zheng, J. Liou, I.-K. Chiang, I. C. Khoo, and T. J. Huang, "All-optical modulation of localized surface plasmon coupling in a hybrid system composed of photo-switchable gratings and Au nanodisk arrays," *J. Phys. Chem. C*, vol. 115, pp. 7717–7722, 2011.
[29] Y. J. Liu, G. Y. Si, E. S. P. Leong, N. Xiang, A. J. Danner, and J. H. Teng, "Light-driven plasmonic color filters by overlaying photoresponsive liquid crystals on gold annular aperture arrays," *Adv. Mater.*, vol. 24, pp. OP131–OP135, 2012.

[30] G. Y. Si *et al.*, "All-optical, polarization-insensitive light tuning properties in silver nanorod arrays covered with photoresponsive liquid crystals," *Phys. Chem. Chem. Phys.*, vol. 17, pp. 13223–13227, 2015.
[31] V. K. S. Hsiao, Y. B. Zheng, B. K. Juluri, and T. J. Huang, "Light-driven plasmonic switches based on au nanodisk arrays and photoresponsive liquid crystals," *Adv. Mater.*, 20, pp. 3528–3532, 2008.
[32] M. Osterfeld, H. Franke, and W. Frank, "Monitoring electric field induced refractive index changes in liquid crystals with polymer lightguides," *Mol. Cryst. Liq. Cryst.*, vol. 183, pp. 321–328, 2006.
[33] C. Menzel, C. Rockstuhl, and F. Lederer, "An advanced Jones calculus for the classification of periodic metamaterials," *Phys. Rev. A*, vol. 82, no. 5, pp. 3464–3467, 2010.
[34] Z. Wang, H. Jia, K. Yao, W. Cai, H. Chen, and Y. Liu, "Circular dichroism metamirrors with near-perfect extinction," *ACS Photon.*, vol. 3, no. 11, pp. 2096–2101, 2016.
[35] D. M. Sullivan, *Electromagnetic Simulation Using the FDTD Method*, 2nd ed. Piscataway, NJ, USA: IEEE Press, 2013.
[36] E. Hecht, *Optics*, 4th ed. Reading, MA, USA: Addison-Wesley, 2002.
[37] P. B. Johnson and R. W. Christy, "Optical constants of the noble metals," *Phys. Rev. B*, vol. 6, pp. 4370–4379, 1972.
[38] M. Kauranen and A. V. Zayats, "Nonlinear plasmonics," *Nature Photon.*, vol. 6, pp. 737–748, 2012.
[39] J. Li, S. T. Wu, S. Brugioni, R. Meucci, and S. Faetti, "Infrared refractive indices of liquid crystals," *J. Appl. Phys.*, vol. 97, 2005, Art. no. 073501.
[40] E. Plum, J. Zhou, J. Dong, V. A. Fedotov, T. Koschny, and C. M. Soukoulis, "Metamaterial with negative index due to chirality," *Phys. Rev. B*, vol. 79, no. 3, 2009, Art. no. 035407.